An experimental investigation on performances recovery of glass fiber reinforced composites exposed to a salt-fog/dry cycle

V. Fiore [a,*], L. Calabrese [b], R. Miranda [a], D. Badagliacco [a], C. Sanfilippo [a], D. Palamara [b], A. Valenza [a], E. Proverbio [b]

[a] Department of Engineering, University of Palermo, Viale delle Scienze, Edificio 6, 90128, Palermo, Italy
[b] Department of Engineering, University of Messina, Contrada Di Dio, Sant'Agata, 98166, Messina, Italy

ARTICLE INFO

ABSTRACT

The main goal of this paper is the evaluation of the properties reversibility of glass fiber reinforced polymers (GFRP$_s$) under discontinuous exposure to aggressive environmental conditions, typical of marine applications. To this aim, the GFRP manufactured through vacuum infusion process has been initially aged in humid conditions (i. e., exposure to salt-fog at 35 °C) for 15 and 30 days and then stored under controlled dry conditions (i.e., 50% R. H. and 23 °C) for times varying between 0 and 21 days. In order to evaluate the recover capability of this material, its water uptake has been monitored along the quasi-static flexural properties during the entire humid/ dry cycle. Moreover, both 3D optical and scanning electron microscopes (SEM) have been used to analyze the morphology of fractured samples at different humid and dry times, thus correlating the properties evolution of the composite with its morphology. The main outcome of the present paper is an evident performances recovery shown by the investigated composite during the drying phase. Indeed, despite its flexural strength and modulus were reduced by about 20% and 10% after 30 days of salt-fog exposition, the GFRP composite evidenced a complete recovery of its initial mechanical performances after long drying times (i.e., 21 days). These findings clearly indicate that although some degradation phenomena occurred during the humid phase, their effects on both strength and stiffness of the investigated composite have proven to be mainly reversible.

1. Introduction

Glass fiber reinforced polymers (GFRPs) are widely used nowadays in several engineering fields such as automotive, buildings and marine thanks to their high good quasi-static and dynamic mechanical properties, low weight, high corrosion resistance and reduced maintenance time and cost [1]. In particular, glass fiber reinforced polymers have been used in the nautical sector since about the 1950s to replace traditional material like metal alloys or wood. Indeed, GRFPs are commonly used as light-weight materials in a wide variety of marine applications such as canoes, boats, ships, fishing trawlers, sonar dome and masts of submarines, low-pressure pipes and storage tanks [2–4]. However, GFRPs involve a very careful engineering and manufacturing design to guarantee a suitable mechanical behavior during their service life. Moreover, a further aspect that needs to be ensured is to offer adequate durability of the composite component while preserving the performance over time regardless of the severe environmental conditions in

which it operates [5,6]. Therefore, numerous research activities have been carried out in the last years to understand better and deeper the aging behavior of GFRP materials as well as to propose developments in their design and manufacture [7–9].

The experimental investigation of the degradative phenomena of GFRPs under accelerated aging conditions represents a well-defined approach that allows to provide effective information to evaluate their mechanical stability over time [10–16]. However, it is essential to consider the conditions that best represent the uncertainty of natural aging under variable environmental conditions [17–19]. At the same time, to minimize the exposure time also preserving the environmental variability, the strategy of proposing aging cycles that integrate different environmental conditions has increasingly developed in recent years [14,20,21].

In this regard, Chilali et al. [22] coupled water aging with loading-unloading cycles, evidencing relevant decreases in the mechanical performances of the aged composites (i.e., about 10% in the

---

stiffness) due to a considerable damage induced by water aging. An analogous approach was proposed by Malloum et al. [23], who evaluated the static and fatigue mechanical properties of flax fiber reinforced composites. The experimental results evidenced that specimens are more sensitive to both fatigue and water ageing phenomena. Cadu et al. [24] highlighted the importance to investigate further the durability issues of composite materials in cyclical environmental conditions.

Aging cycles in which wet or humid phases are followed by dry phases can be considered useful to provide relevant information on materials durability in severe environments that simulate the real operating conditions [25–27].

The relevance of carrying out aging tests by evaluating the effect of absorption and desorption in wet/dry conditions was highlighted by Gunjal et al. [28], who investigated wood plastic composites. Sodoke et al. [29] assessed the effect of wet/dry aging cycles, with duration of up to 104 days, on the mechanical performances of natural fiber reinforced composites with the purpose to understand better the physico-chemical modification due to the applied cyclic aging.

In this context, the opportunity to evaluate the reversible and permanent degradation phenomena occurring during accelerated aging tests was assessed in our previous papers about natural [30] and hybrid composites [31–33]. An added value can be surely represented by a deeper investigation of this issue regarding polymeric materials reinforced by glass fibers: i.e., the most widely used materials for marine applications [34–37]. A further knowledge increase on the material durability under humid/dry cycles could also represent a step forward in the assessment of the degradative phenomena in severe environmental conditions.

To this purpose, the main aim of this research is to evaluate the mechanical performance worsening of GFRP composites and their subsequent recovery, when they are exposed to a humid/dry aging cycle. In particular, three-point bending tests were carried out on woven glass fiber reinforced epoxy composites exposed to salt-fog for 15 and 30 days. Subsequently, a dry phase (i.e., 50% R.H. and 22 °C) at increasing time (i.e., in the range 0–21 days) was performed in order to evidence the performances recovery of the composite when the accelerated aging is interrupted. Furthermore, water uptake and desorption measurements were respectively carried out during humid and dry phases to discriminate the reversible phenomena from the irreversible ones. The morphological analysis of the fractured surfaces of aged and unaged samples was finally performed by using 3D optical and scanning electron microscopies.

2. Experimental part

2.1. Materials and methods

A square GFRP composite panel (350 cm × 350 cm, nominal thickness 3.6 mm) was manufactured through vacuum assisted resin infusion (Fig. 1a) process by using a DEGBA epoxy resin SX8 EVO (Mates Italiana s.r.l., Italy) mixed with its own amine-based hardener (100:30 wt ratio) reinforced with 18 layers of plain weave woven glass fabrics having nominal areal weight of 200 g/m^2 (Mike Compositi, Italy). In accordance with the matrix datasheets, the laminate was first cured at room temperature (25 °C ± 1 °C) for 24 h and then post-cured at 50 °C ± 1 °C for 15 h.

2.2. Salt-fog/dry aging phases

The main goal of this paper consists in the assessment of the mechanical performance reversibility of a GFRP composite aged in humid or wet conditions (such as a marine environment) thanks to a subsequent dry phase.

To this aim, the GFRP composite was at first aged in the salt-fog climatic chamber model SC/KWT 450 by Weiss (Buchen, Germany) for 15 and 30 days, respectively (Fig. 1b). This "humid" phase was carried out according to the ASTM B 117 standard: i.e., by setting the temperature at 35 °C ± 1 °C and by using a 5 wt% NaCl solution (i.e., pH between 6.5 and 7.2) to obtain the salt-fog. In order to avoid the diffusion phenomena in the plane directions thus exalting the water diffusion through the thickness, the entire composite panel was aged in the salt-fog climatic chamber. This choice has allowed to hinder the edge diffusion effect in the composite.

Then, forty samples for each salt-fog exposition time (i.e., 15 and 30 days) were cut to their nominal dimensions (i.e., 13 mm × 64 mm) with the aid of a diamond blade saw. Afterwards, they were stored in a climate-controlled room up to 21 days at 50% ± 10% R.H and 23 °C ± 2 °C ("dry" phase, according to ISO 291:2008 standard, atmosphere class 2), before performing the quasi-static flexural tests (Fig. 1c). In particular, five samples were tested for each dry condition: i.e., 0, 0.5, 1, 2, 3, 7, 11 and 21 days.

All the investigated batches were codified as "G-Wt_hDt_d", where t_h and t_d are numbers referred to the time intervals (expressed in days) of humid and dry phases, respectively. For instance, G-W15D21 code is referred to the batch exposed for 15 days to the salt-fog environment and then dried in controlled conditions for 21 days. Similarly, G-W0D0 is referred to the unaged batch (i.e., reference).
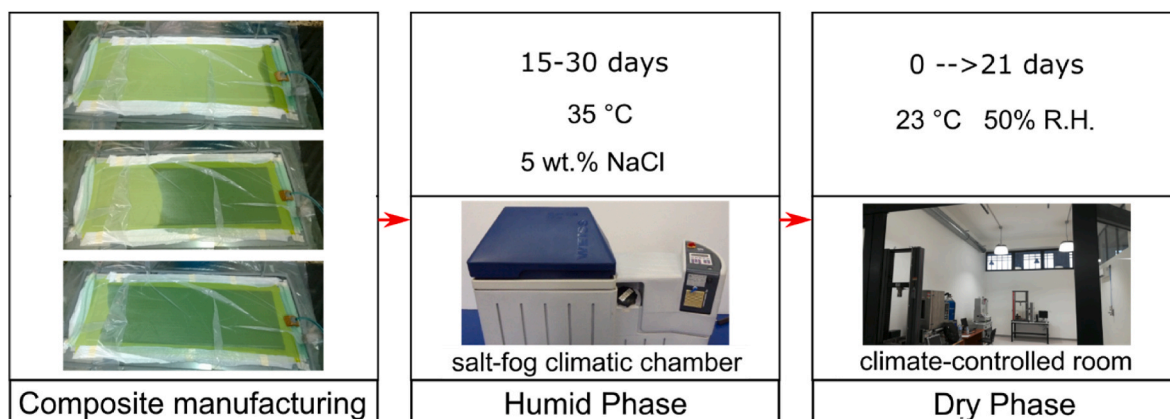

Fig. 1. Flow diagram of the experimental procedure: (a) composite manufacturing, (b) humid phase and (c) dry phase.

2.3. Water uptake

The water uptake was determined at different times during the humid/dry cycle, according to ASTM D570 standard. In particular, two square composite panels (150 mm × 150 mm) were placed in the salt-fog climatic chamber and periodically take out, dried with a clean cloth and finally weighed. Afterwards, the weight of the aged samples was periodically monitored during the dry phase, in order to evaluate the mass recovery capacity of the composite under controlled environmental conditions.

The water uptake (M_t) in percentage was calculated as follows:

$$M_{ti}(\%) = \frac{W_{ti-} W_{t0}}{W_{t0}} \bullet 100 \qquad \text{Eq. 1}$$

Where M_{ti} is the water uptake at the exposure time t_i. Wt_0 and W_{ti} represent the weight of unaged (i.e., at zero time, t_0) and aged (i.e., at time ti) samples, respectively.

Furthermore, in order to investigate the water absorption and desorption properties of the GFRP composite, the diffusion coefficients in the absorption (i.e., humid) and desorption (i.e., dry) phases were determined. Fick's theory is a suitable approach to model the moisture uptake phenomenon and to determine the moisture diffusion coefficients [38]. In particular, based on the Fick's second law of diffusion, the theoretical change in mass (M_t) can be calculated as follows [39]:

$$M_t = \left[1 - \sum_{n=0}^{\infty} \frac{8}{(2n+1)^2 \pi^2} \exp\left(-(2n+1)^2 \pi^2 \frac{D_{ads}t}{h^2} \right) \right] M_\infty \qquad \text{Eq. 2}$$

Where M_∞ is the mass gain (i.e., the water uptake) at saturation, h is the sample thickness, t is the sorption time and D_{ads} is the diffusion coefficient in adsorption. The same approach can be applied also for the desorption process. Hence, the moisture loss during the dry phase can be similarly expressed [39]:

$$M_t - M_\infty = \left[\sum_{n=0}^{\infty} \frac{8}{(2n+1)^2 \pi^2} \exp\left(-(2n+1)^2 \pi^2 \frac{D_{des}t}{h^2} \right) \right] (M_0 - M_\infty) \qquad \text{Eq. 3}$$

Where D_{des} is the diffusion coefficient in desorption. D_{ads} and D_{des} coefficients can be calculated by minimizing the sum of the square error between experimental and theoretical data.

2.4. Density and void content measurements

Density and void content measurements were performed on aged samples before and after the dry phase (i.e., G-W15D0, G-W15D21, G-W30D0 and G-W15D21 batches). Moreover, the same measurements were carried out on unaged samples (i.e., G-W0D0), as a reference. The apparent density (ρ_{ac}) of the composite samples was determined using a helium gas pycnometer (Ultrapyc 5000 foam by Anton Paar, Graz, Austria).

The theoretical density of the composite samples (ρ_{tc}) was calculated based on the simple mixture rule:

$$\rho_{tc} = \frac{1}{\sum_{i=1}^{n} m_i/\rho_i} \qquad \text{Eq. 4}$$

Where, m_i and ρ_i are the weight fraction and density of composite constituents (i.e., epoxy matrix and glass fibers). Furthermore, the voids volume fraction (V_V) of the samples was determined according to ASTM D2734 standard, as follows:

$$V_V = \frac{\rho_{tc} - \rho_{ac}}{\rho_{tc}} \qquad \text{Eq. 5}$$

2.5. Three-point bending tests

For each investigated condition, five prismatic samples (13 mm × 64 mm) were tested under three-point bending configuration by using a U. T.M. model Z005 (Zwick-Roell, Ulm, Germany) equipped with 5 kN load cell. All tests were carried out according to ASTM D790 standard. The support span length was equal to 54 mm and the crosshead speed was set to 1.4 mm/min.

2.6. Morphological analysis

The morphology of the fractured surfaces of samples was analyzed by using a 3D digital optical microscope (KH8700 by Hirox, Tokyo, Japan) and a scanning electron microscopy (ESEM, Quanta 450, FEI, Hillsboro, OR, USA).

3. Results and discussion

3.1. Water absorption/desorption

In order to assess the water absorption and desorption capacities shown by the investigated composite during the humid/dry cycle, the water uptake was monitored at different times during both phases. In this context, Fig. 2 shows the water absorption experienced by G-W15Dx and G-W30Dx batches: i.e., those exposed to the salt-fog spray conditions for 15 and 30 days, respectively. The solid and dashed lines are referred to humid and dry phases, respectively.

By evaluating the effect of the salt-fog exposure (i.e., humid phase), a progressive increase in the composite weight is observed due to the gradual water absorption. The water uptake trend shows a sensible dependence on the exposure time, as evidenced by the initial steep slope of the curve. This implies a weight gain already during the early stages of exposure to the humid environment. In particular, the GFRP composite shows a water uptake equal to 0.38% already after 7 days. A decline in the water uptake trend can be observed over long periods of exposure, which indicates that the composite is progressing towards an equilibrium condition of absorbed water. The maximum water uptake (i.e., ~1.05%) is reached after 30 days of exposure in salt-fog environment (i. e., G-W30 batches). This value is comparable with those observed in similar fiber reinforced polymers [40,41].

Therefore, it was found that the humid phase is marked out by a bimodal trend in the water uptake trend, which evidences a knee at about 15 days. This behavior is attributable to the interaction of various degradation phenomena that synergistically contribute to trigger the progressive water absorption of the composite. In more detail, three main aging steps can be proposed [42,43].
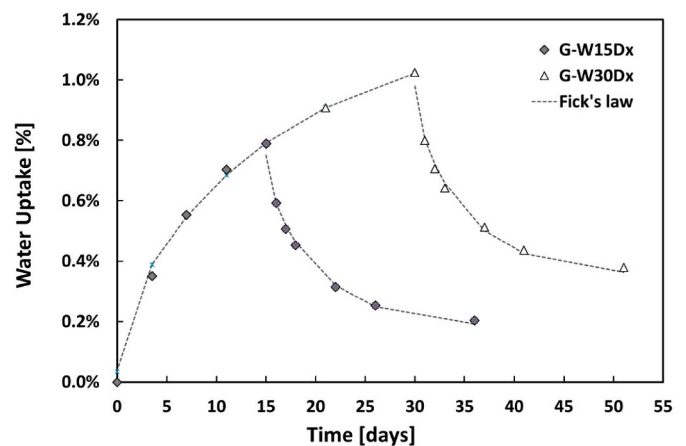
Fig. 2. Water uptake evolution of the GFRP composite at increasing time (dashed and dash-dotted lines are referred to humid phase and dry phases).

- For short exposure time, the water absorption is initially favored by the presence of hydrophilic surface regions [44]. In particular, the water vapor interacts through Van der Waals forces with the polar groups or unreacted hydrophilic areas of the epoxy resin (e.g., amine or hydroxyl terminated groups) forming a thin layer of adsorbed water [45]. The formation of these hydrated colonies in correspondence with the hydrophilic areas of the surface favors the formation of preferential paths for the water diffusion [46,47];
- Subsequently, defects (e.g., micro cavities or voids) on the matrix surface are generated in correspondence of the hydrophilic sites, thus activating the water diffusion within the composite [48]. Furthermore, the distribution of the fibers as well as the resin that surrounds them play a key role in both the absorption kinetic and the water absorbed at saturation [49,50]. In this contest, glass fibers cannot be considered as an active part of the water absorption process. However, superficial degradation phenomena are conceivable due to the interaction between fibers and water, thus inducing local dissolution of the fiber [51,52]. This implies that extra free volumes can be created at the fiber-matrix interface, which speeds up further the water permeation [53];
- Finally, local detachments on the fiber-matrix interface occur due to the progressive water permeation inside the composite [54], Furthermore, possible micro-cracks in the matrix itself (i.e., induced by matrix softening and differential swelling between fiber and matrix) could be identified as additional degradative mechanism [43].

These phenomena are characterized by slow kinetics in addition to being strongly influenced by the presence of superficial or interfacial defects in the composite [55]. The need for extended exposure times to complete the absorption phenomena in a humid environment is validated by considering that long times are required to achieve the water uptake saturation on glass fiber reinforced composites [56]. The absorption curve related to the interval time between 15 and 30 days shows a slope decrease, but no horizontal asymptote is observed, i.e., the water uptake equilibrium is not still reached. This behavior could be associated with the germination of the previously discussed aging phenomena which slowly evolve over time, triggered by the water absorption, thus favoring a slight deviation of the curve from the Fickian behavior [57].

During the dry phase, the composites loss a large amount of the water absorbed with subsequent mass reduction at increasing drying time. For short drying times, a relevant reduction of the water uptake can be observed. In particular, the composite exhibits a weight reduction of ~0.27–0.38% in about 1 day of drying (i.e., by showing weight losses variable from 0.79% to 0.52% for G-W15 batch and from 1.03% to 0.65% for G-W30 batch, respectively).

For longer drying times, the water uptake progressively stabilizes to 0.22% and 0.40% for G-W15 and G-W30 batches, respectively. These low values indicate that most of the water absorbed during the humid phase can be reversibly released during the drying phase. In particular, it was found that about 60–70% of the water absorbed in the humid phase is released during the drying conditioning (i.e., the lowest value is observed for the G-W30 batch, exposed to salt-fog for 30 days).

In order to better assess the capacity of the water molecules to penetrate and to be released by the composite, the diffusion coefficients during both processes (i.e., adsorption and desorption) were calculated by fitting the experimental data with the theoretical equations (2) and (3). The fitting curves are reported in Fig. 2: the dashed line for the humid phase (i.e., adsorption) and the dash-dotted line for the dry phase (i.e., desorption). The results are summarized in Table 1.

The absorption capacity of the composite is characterized by coefficient D_{ads} equal to $9.015 \cdot 10^{-7}$ mm^2/s. This value is about one order of magnitude lower than D_{des}, the desorption diffusion evaluated during the drying phase. The diffusion coefficient in desorption mode was evaluated for both G-W15 and G-W30 batches (i.e., aged in the salt-fog

Table 1
Diffusion parameters in adsorption and desorption.

	M_0 (%)	M_∞ (%)	D (mm^2/s)	Chi-Square
Adsorption	0	1.18	$9.015 \cdot 10^{-7}$	$6.832 \cdot 10^{-8}$
Desorption G-W15	0.77	0.18	$2.667 \cdot 10^{-6}$	$6.236 \cdot 10^{-8}$
Desorption G-W30	1.00	0.35	$2.751 \cdot 10^{-6}$	$7.764 \cdot 10^{-8}$

climatic chamber for 15 and 30 days, respectively). In particular, the D_{des} values during the desorption phase are equal to $2.667 \cdot 10^{-6}$ mm^2/s and to $2.751 \cdot 10^{-6}$ mm^2/s for G-W15 and G-W30 batches, respectively. These results suggest that the water uptake can be defined as the kinetic limiting factor in the humid/drying cycle. Indeed, samples exhibited a rapid weight loss during the dry phase, i.e., significantly higher than the weight gain observed in the same time interval during the humid phase. This behavior can be related to the triggering of local degradative phenomena in the composite (e.g., voids, interfacial debonding, dissolution, etc.) which act as preferential pathways for the migration of the water molecules in the material bulk. These in turns speed up, during the dry phase, the evaporation of the water previously absorbed (i.e., during the humid phase).

The large water amount released during the desorption phase indicates that the water sorption phenomena can be classified as mainly reversible. However, it should be noted that this does not necessarily imply that the phenomena influencing the mechanical performances are fully reversible. Although the presence of voids or cracks created during the humid phase does not involve changes in the residual weight of the composite, they can induce stress concentration zones that trigger premature failures of the samples. Consequently, only the integration of all these information can furnish a more articulated and deeper vision on the reversibility or irreversibility of the degradative processes occurred during the salt-fog exposure of the investigated composite.

Furthermore, with the purpose to assess in more detail the effect of humid/dry aging cycle on the material degradation, Fig. 3 shows the trends of the apparent density and void content of the composite during humid and dry phases.

First of all, slight increases of the apparent density can be observed both after 15 and 30 days of salt-fog exposure. This behavior can be ascribed to the weight gain experienced during the humid phase (see Fig. 2): i.e., the water permeates in the sample cavities (i.e., defects or voids), thus leading to an increase of the composite bulk density [31,58]. In particular, G-W15D0 and G-W30D0 samples showed about 0.19% and 0.23% higher density compared to the unaged one (i.e., G-W0D0, apparent density 1.585 g/cm^3), respectively.

The greater density observed for the samples exposed to the salt-fog for longer times indicates that the primary and secondary water absorption mechanisms become kinetically sensitive with increasing aging
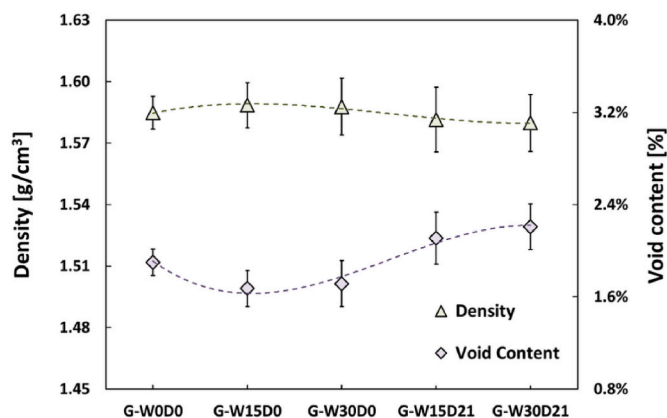

Fig. 3. Density and void content values of the GFRP composite at varying humid and drying conditions.

times. Furthermore, swelling phenomena take place due to absorbed water, which reduce the free volume related to voids, interfacial debonding or cracks generated during the humid phase [59]. Indeed, the void content of the unaged composite (i.e., G-W0D0) is equal to 1.90% whereas the aged samples (i.e., G-W15D0 and G-W30D0) exhibited lower voids amounts (i.e., 1.67% and 1.71%, respectively).

On the contrary, the water absorbed by the samples during the humid phase is released by evaporation in the following dry phase, thus leaving empty the defects and gaps. For this reason, the voids content of the composite increases as well as the bulk density decreases. In particular, G-W15D21 and G-W30D21 samples showed a quite similar bulk density of about 1.58 g/cm^3 whereas, in term of void content, the maximum value (i.e., 2.2%) is shown by G-W30D21 samples (i.e., exposed for 30 days to the salt-fog and then dried for 21 days). It is worth noting that this value is quite similar to that shown by the unaged sample, meaning that the cavities created during the humid phase are not numerous and the triggering of irreversible degradative phenomena (i.e., cracks, delamination and debonding) on the composite should not occur.

3.2. Three-point bending tests

Fig. 4 shows the typical stress-strain curves of unaged (i.e., G-W0D0) and aged samples for different salt-fog exposure times (i.e., G-W15D0 and G-W30D0).

It is possible to notice that, regardless the exposure time, samples exhibit slight reductions in both maximum stress and stiffness (i.e., identified by the slope reduction of the initial linear section of the curve) at the end of the humid phase. In particular, G-W15D0 and G-W30D0 samples exhibited reductions in the average values of the maximum stress equal to −12.5% and −20.4% in comparison to G-W0D0 ones, respectively. At the same time, their average flexural modulus values were found to be −4% and −10.5% lower than unaged samples.

As concerns the strain at break, an overall reduction was evidenced for both batches, mainly due to the premature failure of the aged samples, in turn caused by degradative phenomena occurred during the salt-fog exposure of the composite. Furthermore, G-W15D0 samples showed lower strain at break values in comparison to those exposed to salt-fog for 30 days. This finding can be explained taking into account that the effect of phenomena such as softening and plasticization occurred during the initial humid phase, is more pronounced for longer salt-fog exposure times, thus opposing in a greater extent the strain at break reduction shown by aged samples.

Fig. 5 compares the typical stress-strain curves for samples initially exposed to the salt-fog for 15 days (i.e., G-W15Dx - Fig. 5a) and 30 days
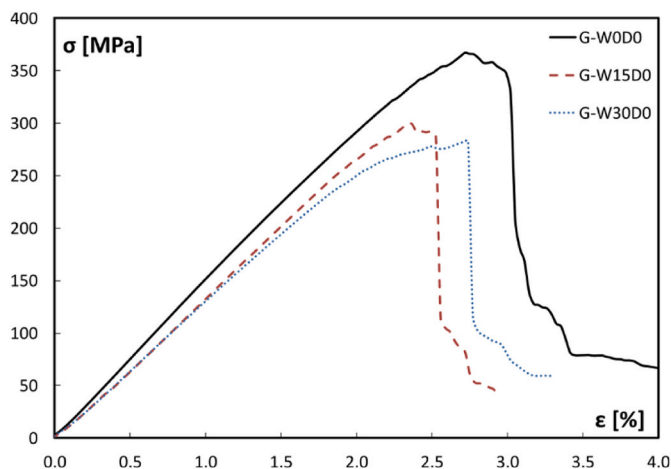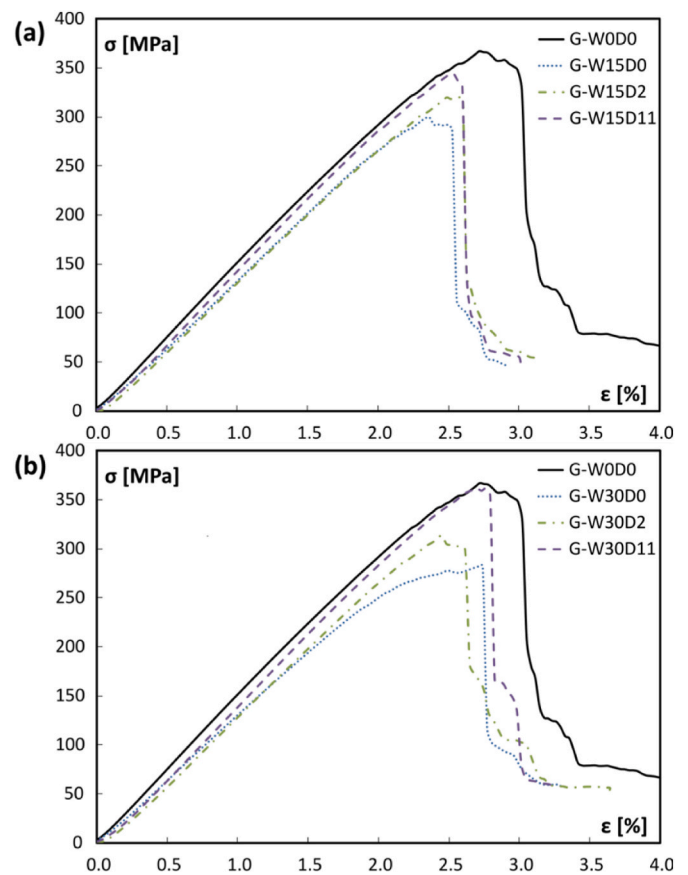

Fig. 5. Typical stress-strain curves at increasing drying time for samples exposed to salt-fog for (a) 15 days (i.e., G-W15Dx batch) and (b) 30 days (i.e., G-W30Dx batch).

(i.e., G-W30Dx - Fig. 5b) and then dried, for different drying times.

By observing this figure, it is possible to notice that the samples storage in dry conditions allows an evident recovery of their mechanical performances. Indeed, Fig. 5a highlights the progressive enhancement of both flexural strength and modulus shown by the GFRP at increasing the drying time. This indicates that the degradative phenomena (e.g., softening, plasticization and so forth) activated during the humid phase cannot be considered permanent or irreversible. The investigated composite is therefore able to recover reversibly its performances after the humid/dry cycle, thus approaching the behavior shown at the beginning of the aging. In particular, G-W15D11 samples (i.e., stored for 11 days at 50% R.H. and 22 °C) show stress-strain curves very similar to that of unaged ones. In particular, it can be noticed that the composite stiffness is fully recovered whereas a slightly lower maximum stress value remains. However, the strain at break values shown by aged samples are lower than unaged ones, regardless the drying time. This behavior could be ascribed to the premature fracture of the composite, triggered by the presence of local defects [60,61] or to the partial polymeric matrix stiffening due to the thermal treatment applied during the salt-fog exposure [62]. Indeed, the humid environmental conditions induce swelling of the polymeric matrices, thus developing internal stresses, which, in turn, favor the formation of micro-cracks or the expansion of pre-existing voids. Furthermore, the composite stiffness can improve when the material is subjected to accelerated aging at medium-high temperatures (i.e., 35 °C in this case) due to the cross-link formation, which develops over time (i.e., post-cure phenomenon).

Similar comments can be made considering how the mechanical response of G-W30Dx samples varies with the drying time (Fig. 5b). In particular, longer aging times in the humid environment amplify the softening effects on the GFRP composite. However, the mechanical

Fig. 4. Typical stress-strain curves for unaged (i.e., G-W0D0) and exposed to salt-fog (i.e., G-W15D0 and G-W30D0) composite samples.

behavior of these samples is progressively recovered during the dry phase (i.e., G-W30D11), similarly to the G-W15Dx batch.

In order to discriminate better how the investigated material modifies its flexural properties during the humid/dry cycle, the evolution of the maximum stress (Fig. 6a) and modulus (Fig. 6b) for G-W15Dx and G-W30Dx batches can be analyzed at different drying times. The red pointed line is referred to the properties of the samples at the end of the humid phase (i.e., without drying). Furthermore, the red dash-dotted line is referred to the unaged batch and can be considered as the threshold value for the assessment of decay and recovery of the mechanical performances of the composite. The error bar related to this value, represented by the gray wavy area, can therefore indicate the lower and upper threshold limits for strength and stiffness in the unaged condition, respectively.

It is possible to notice that both properties show monotonous increases at the end of the humid phase, attributable to their progressive recovery. In particular, this recovery was found to be more marked in the early days of the dry phase. Afterwards, the curve slope progressively decreases until reaching asymptotically the threshold value of the unaged batch. In other words, the composite shows the complete recovery of its initial mechanical performances after long drying times (i.
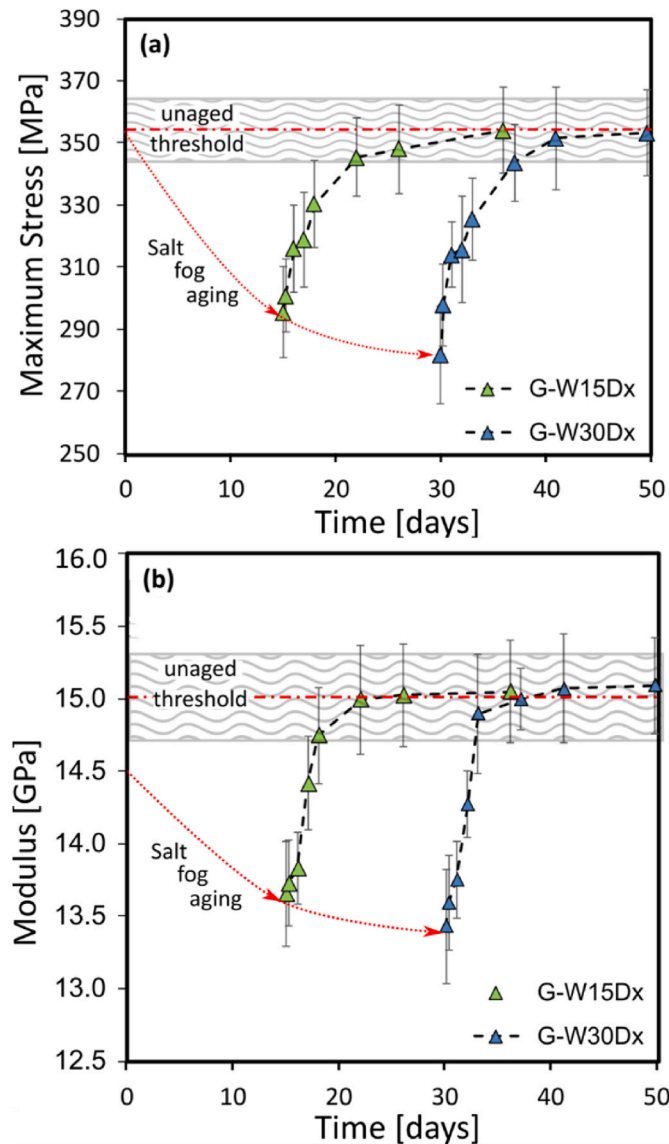
e., 21 days). This can be considered as an unambiguous sign that the degradation phenomena occurred during the humid phase have reversible and non-degenerative effects. The accelerated aging (i.e., salt-fog exposure at 35 °C) actually leads to the weakening and softening of the GFRP composite, as evidenced by the reduction of the mechanical performances experienced by G-W15D0 and G-W30D0 batches. However, this behavior cannot be considered permanent because it is possible to restore the initial performances of the investigated composite by keeping it in a dry environment for an appropriate time. In particular, it is worth of noting that G-W30Dx samples (i.e., exposed to salt-fog for 30 days) show an almost complete recovery of their initial flexural stress and stiffness (i.e., reaching the lower thresholds of the unaged samples) just after 7 and 3 days of drying, respectively.

Further information can be obtained by normalizing the value of a mechanical property (i.e., maximum strength or modulus) shown by the composite at a specific drying time to the related value shown at the beginning of the experimental campaign. Dimensionless indices, correlated to the stiffness or strength recoveries shown by the composite during the dry phase, are therefore derived as follows:

$$FSR = \frac{\sigma_{Dry\_t}}{\sigma_0} \qquad \text{Eq. 6}$$

$$EMR = \frac{E_{Dry\_t}}{E_0} \qquad \text{Eq. 7}$$

Where FSR and EMR indices are defined as the flexural strength ratio and the elastic modulus ratio, respectively. σ_{Dry_t} and E_{Dry_t} are respectively the average values of the flexural strength and modulus shown by the GFRP after a generic drying time t whereas σ_0 and E_0 are the initial values (i.e., shown by the unaged composite) of the same property. These indices are therefore associated with the recovery percentage of the mechanical properties during the dry phase. For instance, an EMR index equal to 0.7 indicates that, after a certain drying time, the aged composite shows an elastic modulus equal to 70% of its initial value, which corresponds to a 30% residual decay in the stiffness. Analogous consideration can be argued for the FSR index, correlated to the maximum flexural stress of the GFRP composite.

Fig. 7 shows the FSR vs EMR plot at different drying times for G-W15Dx and G-W30Dx batches.

As quite predictable, the lowest values of each index are found at the beginning of the dry phase due to the detrimental effect of the salt-fog exposure on the flexural properties of the composite. Moreover, the longer is the humid phase duration, the lower are the FSR and EMR
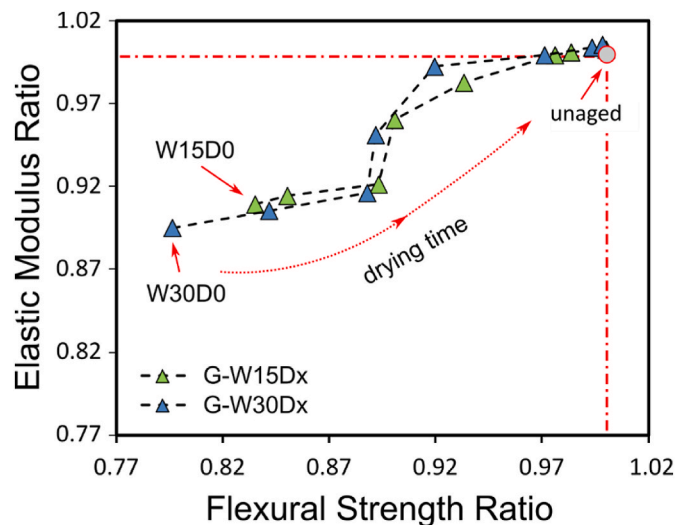

Fig. 6. Evolution of (a) maximum flexural stress and (b) modulus of the GFRP composite at varying the exposition time to humid and dry phases.

Fig. 7. Flexural Strength Ratio (FSR) vs Elastic Modulus Ratio (EMR) at different drying times for G-W15Dx and G-W30Dx batches.

values at the end of this phase. In particular, G-W30D0 samples (i.e., aged in salt-fog for 30 days) show EMR and FSR indices equal to 0.895% and 0.796%, respectively. These results graphically highlight that the flexural strength is more sensitive than modulus to the degradative effects induced by the humid phase.

Afterwards, both indices grow monotonously during the dry phase at increasing the time, with a quite similar trend. This means that both maximum stress and modulus evidence a progressive recovery until they converge to their initial values. In particular, FSR and EMR indices reached their maximum values (i.e., 0.998% and 1.005%, respectively) after 21 days of drying (i.e., G-W30D21 batch). These results made us infer that the elastic modulus and flexural strength are both sensitive to reversible degradative phenomena, which occur and contribute to the performance decrements during the humid phase. It is worth noting that the sigmoidal shape of the curve observable at intermediate drying times indicates the higher ability shown by the investigated composite to recovery its initial stiffness rather than its strength. Indeed, the regain of the latter is kinetically slower: i.e., it needs longer drying times to reach a FSR value close to 100%.

Interesting consideration can be drawn by evaluating the effect of the aging cycle on the fracture morphology of GFRP samples (see bottom and front views shown in Fig. 8).

It can be observed that all samples exhibit catastrophic failures when loaded under three-point bending. As predictable, a tensile crack initially starts in the outer bottom laminae and then it evolves longitudinally to the applied load towards the middle zone of the composite, with no evidence of large debonding or delamination. Finally, the fracture propagates up to the outer upper lamina, which is in contact with the bending punch. The finding that all the samples show similar fracture morphologies (i.e., regardless the humid and dry times) make us infer that the investigated GFRP composite evidences good mechanical stability in these aggressive environmental conditions. No softening phenomenon so relevant to trigger significant changes in the fracture mode have been observed.

In order to evaluate better the possible modifications induced by the humid/dry cycle on the fiber matrix interface, Fig. 9 shows the surfaces' morphology of unaged and aged samples subjected to bending load until complete failure occurred.

These images clearly confirm that the composite morphology did not noticeably change due to the humid/dry cycle. In more detail, a slightly greater interface instability is shown by the aged composites (Fig. 9b) in comparison to unaged ones (Fig. 9a), as evidenced by the presence of few more local fiber/matrix debonding areas. However, these differences are not believed to be enough to induce a significant variation in the composite's mechanical performances at the end of the humid/dry
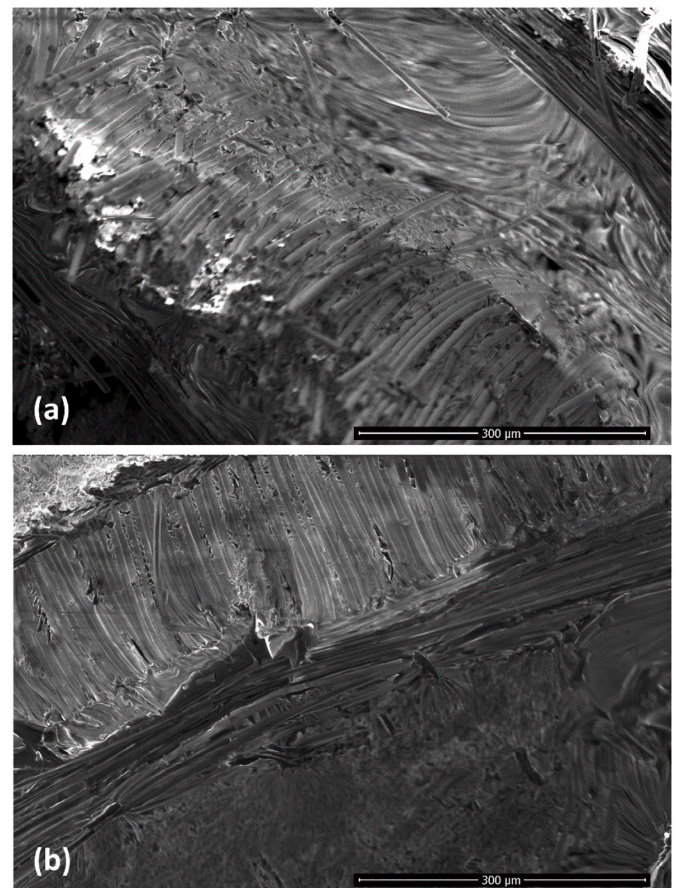

Fig. 9. SEM micrographs of the fractured surfaces of (a) unaged (i.e., G-W0D0) and (b) aged (i.e., G-W30D2) samples.

cycle. Indeed, the close-up observations of the fracture surfaces highlight that the morphologies of unaged (i.e., G-W0D0 shown in Fig. 10a) and aged (i.e., G-W30D2 shown in Fig. 10b) samples are quite similar: i. e., mainly reversible degradative phenomena occurred during the humid phase.

These findings are in fully agreement with the mechanical results. Under salt-fog environmental conditions, the GFRP composite shows a good stability at least up to the investigated exposure time (i.e., 30 days). These promising results, in addition to validating the proposed
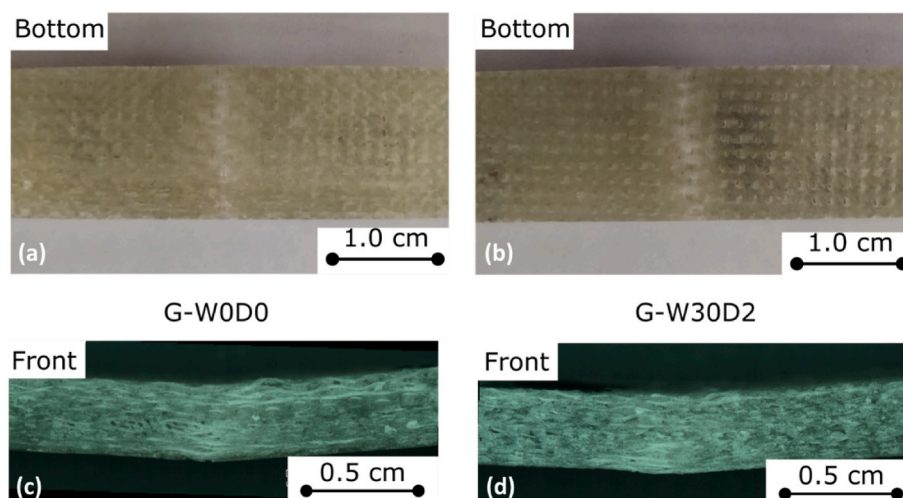

Fig. 8. Views of the in plane and cross section failure mechanisms observed in (a,c) unaged (i.e., G-W0D0) and (b,d) aged (i.e., G-W30D2) composites.
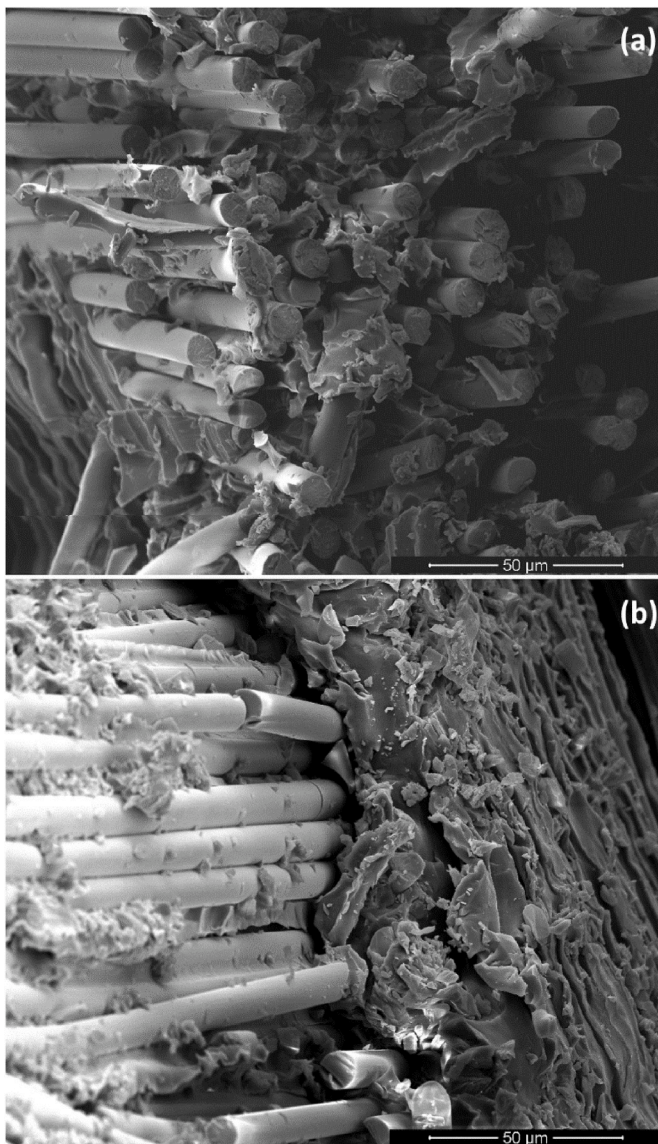
Fig. 10. Close-up micrographs of the fractured surfaces of (a) unaged (i.e., G-W0D0) and (b) aged (i.e., G-W30D2) composites.

experimental approach in terms of potential reversibility of the degradation mechanisms during aging tests, open up new research scenarios aimed to assess the mechanical stability of composite laminates in cyclic aggressive environments. A further aspect of investigation could also be to evaluate the effect of glass fibers hybridization with natural ones, by evaluating as this approach can stimulate the aging reversibility during humid/dry cycles.

4. Conclusion

In this research work, the evaluation of the ability of glass fiber reinforced polymers (GFRPs) to recover its overall performances under discontinuous exposure to aggressive environmental conditions was investigated for the first time. In particular, the investigated composite was subjected to a humid/dry aging cycle, consisting of an initial "humid" phase (i.e., exposure to salt-fog at 35 °C) for 15 and 30 days, followed by a "dry" phase (i.e., 50% R.H. and 23 °C) with duration of up to 21 days. The evolution of the flexural properties of the composite as well as of its water uptake was monitored during both phases. In order to correlate the properties reversibility shown by the composite to the changes in its morphology, the surface of fractured samples was

observed by scanning electron microscope (SEM). By way of summarizing, from the experimental campaign it can be drawn that.

- The GFRP experienced mainly reversible degradative phenomena due to the aging in the salt-fog environment (i.e., humid phase). A progressive performances' recovery was noticed during the dry phase. In particular, a relevant outcome of this paper is that, thanks to the drying step, the composite experienced the recovery of about 100% of their initial flexural strength and stiffness values;
- By defining a topological degradation map related to strength and stiffness worsening, it was possible to highlight that the composite suffered mainly reversible degradative phenomena. This means that the exposure to salt-fog for a limited period of time (i.e., up to 30 days) did not permanently affect the mechanical stability of the investigated composite.

Based on these promising results, possible future research activities will be aimed at comparing the performance stability of full glass, full flax and hybrid glass/flax fiber reinforced composites exposed to humid/dry cycles.

Author statement

V. Fiore, L. Calabrese: Conceptualization, Methodology, Resources, writing - review and editing, Visualization. R. Miranda, D. Badagliacco, C. Sanfilippo: Investigation, Writing - Original Draft. D. Palamara: Investigation, data curation. A. Valenza, E. Proverbio: Supervision, Project administration, Funding acquisition.

Declaration of competing interest

The authors declare that they have no known competing financial interests or personal relationships that could have appeared to influence the work reported in this paper.

Data availability

Data will be made available on request.

Acknowledgements

References

[1] Gu H. Behaviours of glass fibre/unsaturated polyester composites under seawater environment. Mater Des 2009;30:1337–40. https://doi.org/10.1016/j.matdes.2008.06.020.

[2] Kootsookos A, Mouritz AP. Seawater durability of glass- and carbon-polymer composites. Compos Sci Technol 2004;64:1503–11. https://doi.org/10.1016/j.compscitech.2003.10.019.

[3] Nanda T, Singh K, Shelly D, Mehta R. Advancements in multi-scale filler reinforced epoxy nanocomposites for improved impact strength: a review. Crit Rev Solid State Mater Sci 2021;46:281–329. https://doi.org/10.1080/10408436.2020.1777934.

[4] Shelly D, Nanda T, Mehta R. Addition of compatibilized nanoclay and UHMWPE fibers to epoxy based GFRPs for improved mechanical properties. Composer Part A Appl Sci Manuf 2021;145:106371. https://doi.org/10.1016/j.compositesa.2021.106371.

[5] Huera-Huarte FJ, Jeon D, Gharib M. Experimental investigation of water slamming loads on panels. Ocean Eng 2011;38:1347–55. https://doi.org/10.1016/j.oceaneng.2011.06.004.

[6] Bulmanis VN, Gunyaev GM, Krivonos VV, Mashinskaya GP, Merkulova VM, Milyutin GI, et al. Atmospheric durability of polymer-fiber composites in cold climates. Mech Compos Mater 1991;27:698–705. https://doi.org/10.1007/BF00808081.

[7] Sen R. Durability of advanced composites in a marine environment. Int J Mater Prod Technol 2003;19:118–29. https://doi.org/10.1504/IJMPT.2003.003548.

[8] Startsev OV, Blaznov AN, Petrov MG, Atyasova EV. A study of the durability of polymer composites under static loads. Polym Sci Ser D 2019;12:440–8. https://doi.org/10.1134/S1995421219040166.

[9] Fiore V, Calabrese L. Effect of glass fiber hybridization on the durability in salt-fog environment of pinned flax composites. Polymers 2021;13. https://doi.org/10.3390/polym13234201.

[10] Panaitescu I, Koch T, Archodoulaki VM. Accelerated aging of a glass fiber/polyurethane composite for automotive applications. Polym Test 2019;74:245–56. https://doi.org/10.1016/j.polymertesting.2019.01.008.

[11] Chani KS, Saini JS, Bhunia H. Accelerated weathering of bolted joints prepared from woven glass fiber-reinforced nanocomposites. Proc Inst Mech Eng Part L J Mater Des Appl 2019;233:2108–25. https://doi.org/10.1177/1464420719828155.

[12] Calabrese L, Fiore V, Bruzzaniti PG, Scalici T, Valenza A. An aging evaluation of the bearing performances of glass fiber composite laminate in salt spray fog environment. Fibers 2019;7. https://doi.org/10.3390/fib7110096.

[13] Sharma B, Chhibber R, Mehta R. Seawater ageing of glass fiber reinforced epoxy nanocomposites based on silylated clays. Polym Degrad Stabil 2018;147:103–14. https://doi.org/10.1016/j.polymdegradstab.2017.11.017.

[14] Chen Y, Davalos JF, Ray I, Kim HY. Accelerated aging tests for evaluations of durability performance of FRP reinforcing bars for concrete structures. Compos Struct 2007;78:101–11. https://doi.org/10.1016/j.compstruct.2005.08.015.

[15] José-Trujillo E, Rubio-González C, Rodríguez-González JA. Seawater ageing effect on the mechanical properties of composites with different fiber and matrix types. J Compos Mater 2019;53:3229–41. https://doi.org/10.1177/0021998318811514.

[16] Oguz ZA, Erklig A, Bozkurt ÖY. Degradation of hybrid aramid/glass/epoxy composites hydrothermally aged in distilled water. J Compos Mater 2021;55:2043–60. https://doi.org/10.1177/0021998320984237.

[17] Hota G, Barker W, Manalo A. Degradation mechanism of glass fiber/vinylester-based composite materials under accelerated and natural aging. Construct Build Mater 2020;256. https://doi.org/10.1016/j.conbuildmat.2020.119462.

[18] Gasem ZM. Long-term natural aging effects on flexural properties of E-glass/vinyl ester filament-wound pipes. Arabian J Sci Eng 2022. https://doi.org/10.1007/s13369-022-06930-2.

[19] Viña J, Bonhomme J, Mollón V, Viña I, Argüelles A. Mechanical properties of fibreglass and carbon-fibre reinforced polyetherimide after twenty years of outdoor environmental aging in the city of Gijón (Spain). Compos Commun 2020;22. https://doi.org/10.1016/j.coco.2020.100522.

[20] Mouzakis DE, Zoga H, Galiotis C. Accelerated environmental ageing study of polyester/glass fiber reinforced composites (GFRPCs). Compos B Eng 2008;39:467–75. https://doi.org/10.1016/j.compositesb.2006.10.004.

[21] Shao Y, Dong Y, Yang Y. Effect of low-cycle fatigue and hydrothermal aging on tensile properties of open-hole glass fiber/polycarbonate and glass fiber/polyamide 6 composites. Fibers Polym 2021;22:2527–34. https://doi.org/10.1007/s12221-021-1228-y.

[22] Chilali A, Zouari W, Assarar M, Kebir H, Ayad R. Effect of water ageing on the load-unload cyclic behaviour of flax fibre-reinforced thermoplastic and thermosetting composites. Compos Struct 2018;183:309–19. https://doi.org/10.1016/J.COMPSTRUCT.2017.03.077.

[23] Malloum A, Mahi A El, Idriss M. The effects of water ageing on the tensile static and fatigue behaviors of greenpoxy–flax fiber composites. J Compos Mater 2019;53:2927–39. https://doi.org/10.1177/0021998319835596.

[24] Cadu T, Van Schoors L, Sicot O, Moscardelli S, Divet L, Fontaine S. Cyclic hygrothermal ageing of flax fibers' bundles and unidirectional flax/epoxy composite. Are bio-based reinforced composites so sensitive? Ind Crop Prod 2019;141:111730. https://doi.org/10.1016/j.indcrop.2019.111730.

[25] Neşer G. Polymer based composites in marine use: history and future trends. Procedia Eng 2017;194:19–24. https://doi.org/10.1016/j.proeng.2017.08.111.

[26] Mak K, Fam A. The effect of wet-dry cycles on tensile properties of unidirectional flax fiber reinforced polymers. Compos B Eng 2020;183:107645. https://doi.org/10.1016/j.compositesb.2019.107645.

[27] Gao C, Zhou C. Moisture absorption and cyclic absorption–desorption characters of fibre-reinforced epoxy composites. J Mater Sci 2019;54:8289–301. https://doi.org/10.1007/s10853-019-03399-7.

[28] Gunjal J, Abhilash RM, Chauhan SS. Effect of repeated cycles of wetting and drying on mechanical properties of wood–polypropylene composites. J Indian Acad Wood Sci 2020;17:114–22. https://doi.org/10.1007/s13196-020-00262-0.

[29] Sodoke FK, Toubal L, Laperrière L. Wetting/drying cyclic effects on mechanical and physicochemical properties of quasi-isotopic flax/epoxy composites. Polym Degrad Stabil 2019;161:121–30. https://doi.org/10.1016/j.polymdegradstab.2019.01.014.

[30] Fiore V, Calabrese L, Miranda R, Badagliacco D, Sanfilippo C, Palamara D, et al. On the response of flax fiber reinforced composites under salt-fog/dry conditions: reversible and irreversible performances degradation. Compos B Eng 2022;230:109535. https://doi.org/10.1016/j.compositesb.2021.109535.

[31] Fiore V, Calabrese L, Miranda R, Badagliacco D, Sanfilippo C, Palamara D, et al. Assessment of performance degradation of hybrid flax-glass fiber reinforced epoxy composites during a salt spray fog/dry aging cycle. Compos B Eng 2022;238. https://doi.org/10.1016/j.compositesb.2022.109897.

[32] Calabrese L, Fiore V, Piperopoulos E, Badagliacco D, Palamara D, Valenza A, et al. In situ monitoring of moisture uptake of flax fiber reinforced composites under humid/dry conditions. J Appl Polym Sci 2021. https://doi.org/10.1002/app.51969. n/a:51969.

[33] Calabrese L, Fiore V, Miranda R, Badagliacco D, Sanfilippo C, Palamara D, et al. Performances recovery of flax fiber reinforced composites after salt-fog aging test. J Compos Sci 2022;6:1–12. https://doi.org/10.3390/jcs6090264.

[34] Di Bella G, Calabrese L, Borsellino C. Mechanical characterisation of a glass/polyester sandwich structure for marine applications. Mater Des 2012;42:486–94. https://doi.org/10.1016/j.matdes.2012.06.023.

[35] Gellert EP, Turley DM. Seawater immersion ageing of glass-fibre reinforced polymer laminates for marine applications. Composer Part A Appl Sci Manuf 1999;30:1259–65. https://doi.org/10.1016/S1359-835X(99)00037-8.

[36] Agarwal P, Kumar M, Sharma A, Choudhary M, Shekhawat D, Patnaik A. Experimental and numerical investigation on slurry erosion performance of hybrid glass/steel fiber reinforced polymer composites for marine applications. Polym Compos 2022;43:5592–610. https://doi.org/10.1002/pc.26874.

[37] Garg M, Sharma S, Mehta R. Carbon nanotube-reinforced glass fiber epoxy composite laminates exposed to hygrothermal conditioning. J Mater Sci 2016;51:8562–78. https://doi.org/10.1007/s10853-016-0117-z.

[38] Grammatikos SA, Zafari B, Evernden MC, Mottram JT, Mitchels JM. Moisture uptake characteristics of a pultruded fibre reinforced polymer flat sheet subjected to hot/wet aging. Polym Degrad Stabil 2015;121:407–19. https://doi.org/10.1016/j.polymdegradstab.2015.10.001.

[39] Yu X, Schmidt AR, Bello-Perez LA, Schmidt SJ. Determination of the bulk moisture diffusion coefficient for corn starch using an automated water sorption instrument. J Agric Food Chem 2008;56:50–8. https://doi.org/10.1021/jf071894a.

[40] Gibhardt D, Doblies A, Meyer L, Fiedler B. Effects of hygrothermal ageing on the interphase, fatigue, and mechanical properties of glass fibre reinforced epoxy. Fibers 2019;7. https://doi.org/10.3390/fib7060055.

[41] Rocha IBCM, Raijmaekers S, van der Meer FP, Nijssen RPL, Fischer HR, Sluys LJ. Combined experimental/numerical investigation of directional moisture diffusion in glass/epoxy composites. Compos Sci Technol 2017;151:16–24. https://doi.org/10.1016/j.compscitech.2017.08.002.

[42] Assarar M, Scida D, El Mahi A, Poilâne C, Ayad R. Influence of water ageing on mechanical properties and damage events of two reinforced composite materials: flax-fibres and glass-fibres. Mater Des 2011;32:788–95. https://doi.org/10.1016/j.matdes.2010.07.024.

[43] Moudood A, Rahman A, Khanlou HM, Hall W, Öchsner A, Francucci G. Environmental effects on the durability and the mechanical performance of flax fiber/bio-epoxy composites. Compos B Eng 2019;171:284–93. https://doi.org/10.1016/j.compositesb.2019.05.032.

[44] Sauro S, Watson TF, Tay FR, Chersoni S, Breschi L, Bernardi F, et al. Water uptake of bonding systems applied on root dentin surfaces: a SEM and confocal microscopic study. Dent Mater 2006;22:671–80. https://doi.org/10.1016/j.dental.2005.08.006.

[45] Perrin FX, Nguyen MH, Vernet JL. Water transport in epoxy–aliphatic amine networks – influence of curing cycles. Eur Polym J 2009;45:1524–34. https://doi.org/10.1016/j.eurpolymj.2009.01.023.

[46] Zhou J, Lucas JP. Hygrothermal effects of epoxy resin. Part I: the nature of water in epoxy. Polymer 1999;40:5505–12. https://doi.org/10.1016/S0032-3861(98)00790-3.

[47] Karad SK, Attwood D, Jones FR. Moisture absorption by cyanate ester modified epoxy resin matrices. Part V: effect of resin structure. Composer Part A Appl Sci Manuf 2005;36:764–71. https://doi.org/10.1016/j.compositesa.2004.10.022.

[48] Almudaihesh F, Holford K, Pullin R, Eaton M. A comparison study of water diffusion in unidirectional and 2D woven carbon/epoxy composites. Polym Compos 2022;43:118–29. https://doi.org/10.1002/pc.26361.

[49] Joliff Y, Rekik W, Belec L, Chailan JF. Study of the moisture/stress effects on glass fibre/epoxy composite and the impact of the interphase area. Compos Struct 2014;108:876–85. https://doi.org/10.1016/j.compstruct.2013.10.001.

[50] Bond DA. Moisture diffusion in a fiber-reinforced composite: Part I – non-fickian transport and the effect of fiber spatial distribution. J Compos Mater 2005;39:2113–41. https://doi.org/10.1177/0021998305052030.

[51] Wei B, Cao H, Song S. Degradation of basalt fibre and glass fibre/epoxy resin composites in seawater. Corrosion Sci 2011;53:426–31. https://doi.org/10.1016/j.corsci.2010.09.053.

[52] Garcia-Espinel JD, Castro-Fresno D, Parbole Gayo P, Ballester-Muñoz F. Effects of sea water environment on glass fiber reinforced plastic materials used for marine civil engineering constructions. Mater Des 2015;66:46–50. https://doi.org/10.1016/j.matdes.2014.10.032.

[53] Stamboulis A, Baillie CA, Peijs T. Effects of environmental conditions on mechanical and physical properties of flax fibers. Composer Part A Appl Sci Manuf 2001;32:1105–15. https://doi.org/10.1016/S1359-835X(01)00032-X.

[54] Dhakal HN, Zhang ZY, Richardson MOW. Effect of water absorption on the mechanical properties of hemp fibre reinforced unsaturated polyester composites. Compos Sci Technol 2007;67:1674–83. https://doi.org/10.1016/j.compscitech.2006.06.019.

[55] Prolongo SG, Gude MR, Ureña A. Water uptake of epoxy composites reinforced with carbon nanofillers. Composer Part A Appl Sci Manuf 2012;43:2169–75. https://doi.org/10.1016/j.compositesa.2012.07.014.

[56] Rocha IBCM, Raijmaekers S, Nijssen RPL, van der Meer FP, Sluys LJ. Hygrothermal ageing behaviour of a glass/epoxy composite used in wind turbine blades. Compos Struct 2017;174:110–22. https://doi.org/10.1016/j.compstruct.2017.04.028.

[57] Mercier J, Bunsell A, Castaing P, Renard J. Characterisation and modelling of aging of composites. Composer Part A Appl Sci Manuf 2008;39:428–38. https://doi.org/10.1016/j.compositesa.2007.08.015.

[58] Castro López C, Lefebvre X, Brusselle-Dupend N, Klopffer M-H, Cangémi L, Castagnet S, et al. Effect of porosity and hydrostatic pressure on water absorption in a semicrystalline fluoropolymer. J Mater Sci 2016;51:3750–61. https://doi.org/10.1007/s10853-015-9692-7.

[59] Saw SK, Akhtar K, Yadav N, Singh AK. Hybrid composites made from jute/coir fibers: water absorption, thickness swelling, density, morphology, and mechanical properties. J Nat Fibers 2014;11:39–53. https://doi.org/10.1080/15440478.2013.825067.

[60] Wang K, Chen Y, Long H, Baghani M, Rao Y, Peng Y. Hygrothermal aging effects on the mechanical properties of 3D printed composites with different stacking sequence of continuous glass fiber layers. Polym Test 2021;100. https://doi.org/10.1016/j.polymertesting.2021.107242.

[61] Grammatikos SA, Evernden M, Mitchels J, Zafari B, Mottram JT, Papanicolaou GC. On the response to hygrothermal aging of pultruded FRPs used in the civil engineering sector. Mater Des 2016;96:283–95. https://doi.org/10.1016/j.matdes.2016.02.026.

[62] Marouani S, Curtil L, Hamelin P. Ageing of carbon/epoxy and carbon/vinylester composites used in the reinforcement and/or the repair of civil engineering structures. Compos B Eng 2012;43:2020–30. https://doi.org/10.1016/j.compositesb.2012.01.001.